2009 American Control Conference
Hyatt Regency Riverfront, St. Louis, MO, USA
June 10-12, 2009

An Optimal Control Model for Human Postural Regulation

Yao Li *Student Member*, *IEEE*, and William S. Levine, *Fellow, IEEE*

***Abstract*—This paper proposes a convex optimal control problem as a mathematical model of human postural control during quiet standing. The human body is modeled as a two-segment inverted pendulum controlled by a single ankle torque. Several performance criteria that are quartic in the state and quadratic in the control are utilized. The discrete-time approximation to each of these problems is a convex programming problem. These problems were solved by the Newton-KKT method. The solutions are shown to exhibit many of the experimentally observed postural control phenomena, especially greater sway than would occur with a linear feedback control without delay.**

I. Introduction

HUMAN postural control has been extensively studied over many years, primarily because understanding the postural control system would likely lead to better means of protecting people from falls—a major threat to the elderly [12][20]. Nonetheless, there are still relatively simple aspects of the control that are poorly understood and somewhat controversial. Specifically, humans standing quietly seem to sway more than is consistent with a linear feedback controller with no feedback delay [19] . Because the sway amplitude is small, linearization of the closed–loop dynamics is certainly appropriate, so it is hard to image that nonlinearities in the control are important during postural sway.

However, a nonlinear controller that is approximately linear with zero gain at the nominal equilibrium posture could possibly explain postural sway. It is also reasonable to believe that the human postural control system is, in some sense, optimal. We hypothesize that the performance measure is not linear quadratic (LQ) but is of higher order (HO), i.e., the performance measure has the form

$$J = \frac{1}{2}\int_0^\infty [\sum_{i=1}^{K} q_i x_i^{2m}(t) + \sum_{j=1}^{L} r_j u_j^2(t)]dt \qquad (1)$$

where q_i and r_j are cost coefficients, K,L,m are integers, and the x_i and u_j are deviations from the nominal equilibrium values of the states and controls respectively. The rest of this paper is devoted to testing this hypothesis.

William S. Levine is with the Department of Electrical and Computer Engineering, University of Maryland at College Park. MD, USA 20740 (Phone: +301-405-3654, Email: wsl@umd.edu)

Yao Li is with the Department of Electrical and Computer Engineering, University of Maryland at College Park. MD, USA 20740 (Phone: +301-405-3654, Email: yaoli@umd.edu)

The following section reviews the prior literature on postural control. This is followed by a derivation of the model of the quietly standing human, which, although simple, is standard in the literature. The resulting optimal control problem is then described, discretized and solved for four versions of the performance criteria. The solutions to the optimal control problems with higher order (HO) performance criteria are shown to exhibit several characteristic features of quietly standing humans. The paper concludes with a description of three specific important and straightforward ways in which this research can be extended.

II. Background

Many early works have investigated different aspects of the quantitative and qualitative properties of the spontaneous postural sway: proprioception [7][16], vestibular system [15], vision [1][4][8] and somato-sensory [9][10][11]. Postural sway during quiet standing is influenced by different physiological conditions, including: aging [1] height, weight, and muscle strength/weakness as well as disease state [19]. Postural sway is inconsistent with the usual feedback controls in engineering because it is spontaneous with low amplitude and low energy consumption. Many quantitative and qualitative analyses of spontaneous postural sway have been performed in the time and frequency domain to characterize the random oscillatory motions including: trajectory of the center of pressure (CP) [4][5][6][15][16]; trajectory of the center of mass (CM) [21][22]; trajectory of the ankle joint angle [7][8] and trajectories of other body points [1][2]. Sway amplitude and velocity are the two most important measurements to characterize the anterior-posterior postural sway behavior.

Collins and DeLuca[5] proposed a combination of open- and closed-loop control strategies and introduced a new analysis technique called the Stabilogram Diffusion Function (SDF) to explain their experimental findings. SDF measures the similarity of the average center of pressure (CP) between different time intervals. This analysis is very sensitive to sway amplitude and velocity; it showed that quiet stance behavior is characterized by "persistence" over short time intervals and "anti-persistence" over longer time intervals.

For a long time, standing posture control strategies were considered to be reflex-like responses elicited automatically by a sensory stimulus. But now it is more commonly believed to be a fundamental motor skill learned by the central nervous system (CNS). The idea is that the CNS anticipates

978-1-4244-4524-0/09/$25.00 ©2009 AACC

spontaneous changes in body position during quiet stance and continuously modulates ankle extensor muscle activity to compensate for the changes. The behavior of the postural control system has been approximated by various linear systems with multiple parameters including:1) Linear (P/PD/ PID) Control[19]; 2) LQR[13]. The parameters have included muscle stiffness, damping, time delay and a source of random noise, etc.

III. Normalized Human Upright Standing Model

A. Inverted Pendulum Model

The human body is often approximated and simplified as a single segment, single joint inverted pendulum that rotates about the ankle joint. This model has been widely used in studying standing posture control during quite upright standing [17][18][21]. One reason for this is that experimental observations suggest that, for small postural deviations, there is very little, if any, knee and hip angular motion. We use this simple model here, although it should be obvious that our approach also applies to much more complex and realistic multi-segment models of the quietly standing human

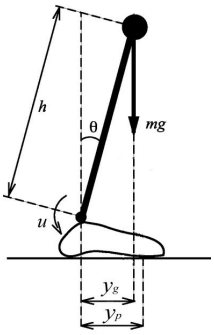

Figure 1. Single joint inverted pendulum model used in studying posture control during quite upright standing

The dynamical equation for the inverted-pendulum is

$$I_o \frac{d^2\theta}{dt} = Mghsin(\theta) + u + \epsilon \tag{2}$$

θ	Sway angle
$\dot{\theta}$	Sway velocity
$\ddot{\theta}$	Sway acceleration
M	The body segment mass
I_o	Moment of inertia of the body segment
h	Distance of CM from the ankle
g	Acceleration of gravity
u	Total ankle torque
y_g	Horizontal displacement of the CM
y_p	Horizontal displacement of the CP
ϵ	Disturbance torque

In this inverted pendulum model, ankle torque is the control input. The ankle joint torque that stabilizes the body during quiet stance can be generated actively and passively. Passive torque [17] components are the result of tension/stiffness produced by muscle tonus and by the stiffness of the surrounding tissue, such as ligaments and tendons. The active torque [17] component is produced by muscle contractions. Because the CM is located in front of the ankle joint, backward ankle torque is continuously applied to the body to prevent it from falling forward [20]. However, the stabilization of quiet stance by passive torque alone is not possible, and therefore an active component is required to maintain stability.

Because ankle flexor activity is rare and ankle extensors are considerably activated, it can be said that ankle extensors contribute the most toward control of the ankle joint torque and therefore the body posture during quiet stance. [12].

B. Dimensional Analysis

Dimensional analysis has been often used for qualitative reasoning about physical systems. For this human standing model $[\cdot]$ denotes dimension, M is mass, L is length, T is time and 1 indicates dimensionless.

$$\begin{array}{ll} [\theta] = 1 & [I_o] = ML^2 \\ [g] = L/T^2 & [h] = L \\ [u] = ML^2/T^2 & [\epsilon] = ML^2/T^2 \end{array}$$

We introduce the quantities

$$\tilde{\theta}(\tau) = \theta(t),\ \tilde{u}(\tau) = u(t),\ \tilde{\epsilon}(\tau) = \epsilon(t) \tag{3}$$

where $\tau = t/\beta$ and the normalization factor $\beta = \sqrt{h/g}$, which has dimension $[\beta] = T$. Given $\frac{dt}{d\tau} = \beta$ and $\tilde{\theta}(\tau) = \theta(t)$, we apply the chain rule to obtain a dimensionless first order derivative with respective to time $\frac{d\tilde{\theta}(\tau)}{d\tau} = \beta\frac{d\theta(t)}{dt}$. Repeating the process for the second derivative:

$$\frac{d^2\tilde{\theta}(\tau)}{d\tau^2} = \beta^2\frac{d^2\theta(t)}{dt^2} \tag{4}$$

Now, we can rewrite Equation (2)

$$I_o\frac{1}{\beta^2}\frac{d^2\tilde{\theta}(\tau)}{d\tau^2} = mghsin\tilde{\theta}(\tau) + \tilde{u}(\tau) + \tilde{\epsilon}(\tau) \tag{5}$$

Given $\beta = \sqrt{h/g}$, we have

$$\frac{d^2\tilde{\theta}(\tau)}{d\tau^2} = \frac{mgh}{I_o}\frac{h}{g}sin\tilde{\theta}(\tau) + \frac{\tilde{u}(\tau)}{I_o}\frac{h}{g} + \frac{\tilde{\epsilon}(\tau)}{I_o}\frac{h}{g} \tag{6}$$

Let $\frac{mgh}{I_o} = \alpha$. We can simplify Equation (6) into a completely dimensionless form:

$$\frac{d^2\tilde{\theta}(\tau)}{d\tau^2} = \alpha\beta^2 sin\tilde{\theta}(\tau) + \frac{\tilde{u}(\tau)}{I_o}\beta^2 + \frac{\tilde{\epsilon}(\tau)}{I_o}\beta^2 \tag{7}$$

It is interesting to notice: $[\alpha] = \frac{1}{T^2}$, whereas $[\beta^2] = T^2$ and dimensions of each variable are $\left[\frac{d^2\tilde{\theta}(\tau)}{d\tau^2}\right] = 1$, $\left[\tilde{\theta}(\tau)\right] = 1$, $\left[\alpha\beta^2\right] = 1$, $\left[\frac{\tilde{u}(\tau)}{I_o}\beta^2\right] = 1$ and $\left[\frac{\tilde{\epsilon}(\tau)}{I_o}\beta^2\right] = 1$. We omit the tilde and simplify as,

$$\ddot{\theta}(\tau) = \alpha\beta^2 sin\theta(\tau) + \frac{u(\tau)}{I_o}\beta^2 + \frac{\epsilon(\tau)}{I_o}\beta^2 \tag{8}$$

then, letting $\hat{x}_1 = \theta$, $\hat{x}_2 = \dot{\theta}$

$$\begin{cases} \dot{\hat{x}}_1 = \hat{x}_2 \\ \dot{\hat{x}}_2 = \alpha\beta^2 sin(\hat{x}_1) + \frac{u(\tau)}{I_o}\beta^2 + \frac{\epsilon(\tau)}{I_o}\beta^2 \end{cases} \tag{9}$$

Further define $\hat{u} = \frac{u}{I_0}\beta^2$, $\hat{\epsilon} = \frac{\epsilon(\tau)}{I_o}\beta^2$ and a nominal equilibrium posture of $\hat{x}_1 = 10^\circ$, $\hat{x}_2 = 0$. We can then apply $sin(\hat{x}_1 - 10) \rightsquigarrow \hat{x}_1 - 10$ to simplify the system without losing generality, because the angular excursions possible during stable posture regulation are less than $\pm 5^o$. Then the dimensionless differential Equation (9) linearized about $\hat{x}_1 = 10^\circ$, $\hat{x}_2 = 0$ has the simplified form :

$$\begin{cases} \dot{x}_1 = x_2 \\ \dot{x}_2 = \alpha\beta^2 x_1 + \hat{u} + \hat{\epsilon} \end{cases} \tag{10}$$

where x_1 and x_2 are deviations from the nominal equilibrium point and $\hat{u}$ is defined as the difference from the $\hat{u}$ needed to maintain equilibrium at 10°. The two parameters α and β provide a body characteristic measurement for the sway model.

C. Performance Measure

Since the prior research suggests the postural controller is fairly insensitive to small errors, the plant model has two states and one controller, and the noise is very small, we (temporarily) ignore the noise and simplify Eqn (1) to

$$J = \frac{1}{2}\int_0^\infty [px_1^{2m}(t) + qx_2^{2n}(t) + \hat{u}^2(t)]dt \tag{11}$$

As m and n increase, the performance measure assigns smaller and smaller weight to small postural sway. We will discuss the choice of p, q, m and n below.

IV. Solution of Optimal Control Problem

Discretization

We define $\underline{x} = \begin{bmatrix} x_1 \\ x_2 \end{bmatrix}$, coefficient $A = \begin{bmatrix} 0 & 1 \\ \alpha\beta^2 & 0 \end{bmatrix}$ and $B = \begin{bmatrix} 0 \\ 1 \end{bmatrix}$. By choosing the discrete time step $\hat{\tau}$ we can convert the continuous-time system in Eqn (10) to the discrete time system:

$$\begin{aligned} \underline{x}(k+1) - \underline{x}(k) = {} & \tfrac{\hat{\tau}}{2}[A\underline{x}(k+1) + B\hat{u}(k+1)] \\ & + \tfrac{\hat{\tau}}{2}[A\underline{x}(k) + B\hat{u}(k)] \end{aligned}$$

Let $\overline{A} = \begin{bmatrix} 0 & \frac{\tau}{2} \\ \alpha\beta^2\frac{\tau}{2} & 0 \end{bmatrix}$ and $\overline{B} = \begin{bmatrix} 0 \\ \frac{\tau}{2} \end{bmatrix}$. Then, the discrete time optimal control problem is defined as

$$\begin{aligned} &\textbf{min } J(\underline{x}, \hat{u}) = \textstyle\sum_0^N px_1^{2m}(k) + qx_2^{2n}(k) + \hat{u}^2(k) \\ &\textbf{subject to } \underline{x}(k+1) = \tilde{A}\underline{x}(k) + \tilde{B}[\hat{u}(k+1) + \hat{u}(k)] \end{aligned}$$

where

$$\tilde{A} = (I - \overline{A})^{-1}(I + \overline{A}) \ , \ \tilde{B} = (I - \overline{A})^{-1}\overline{B}$$

and N is the final time for the optimal control. This is always a convex programming problem. Such problems are known to have a solution and are comparatively easy to solve using a Newton-KKT interior point method.

Define new overall optimization variable

We introduce a new overall optimization variable as

$$\underline{s} = [\hat{u}(0), \underline{x}(1)^T, \hat{u}(1), \underline{x}(2)^T, \hat{u}(2) \ldots, \underline{x}(N)^T, \hat{u}(N)]^T$$

The objective function $J(\underline{x}, \hat{u})$ then becomes $J(\underline{s})$ and the variable $\underline{s} \in \mathbb{R}^{3N+1}$. We introduce the following notation for the Newton-KKT iteration algorithm.

$\underline{s}^{(i)}$	Overall state variable at i^{th} iteration
$\underline{r}^{(i)}$	Gradient for the overall state variable at i^{th} iteration, defined as $\underline{r}^{(i)} = \nabla J(\underline{s}^{(i)})$
$H^{(i)}$	Hessian matrix for overall state variable at i^{th} iteration, defined as $H^{(k)} = \nabla^2 J(\underline{s}^{(i)})$

Note that the Hessian $H^{(i)}$ is block diagonal.

$$H^{(i)} = diag[R_0^{(i)}, Q_1^{(i)}, R_1^{(i)}, Q_2^{(i)}, R_2^{(i)}, \ldots Q_N^{(i)}, R_N^{(i)}]$$

where

$$R_n^{(i)} = \nabla^2 f(\hat{u}_n^{(i)}) = 2$$
$$Q_n^{(i)} = \nabla^2 f(\underline{x}_n^{(i)}) = \begin{bmatrix} \frac{\partial^2 f(\underline{x}_n^{(i)})}{\partial x_1 \partial x_1} & 0 \\ 0 & \frac{\partial^2 f(\underline{x}_n^{(i)})}{\partial x_2 \partial x_2} \end{bmatrix}$$

Each term on the diagonal of the Hessian $H^{(i)} = \nabla^2 J(\underline{s}^{(i)})$ is positive definite, except at $x_1(k) = 0$ or $x_2(k) = 0$ for some $k = 0, 1, 2, ..., N$.

Newton-KKT Interior-Point Methods

In this section, we describe an iterative interior point algorithm to solve the KKT system [3]. The Newton step $\triangle\underline{s}_{nt}^{(i)}$ for an equality constrained problem is characterized by the following KKT system:

$$\begin{bmatrix} H^{(i)} & A_s^T \\ A_s & 0 \end{bmatrix} \begin{bmatrix} \triangle\underline{s}_{nt}^{(i)} \\ \underline{w} \end{bmatrix} = \begin{bmatrix} -\underline{r}^{(i)} \\ 0 \end{bmatrix} \tag{12}$$

where

$$A_s = \begin{bmatrix} -\tilde{B} & I & -\tilde{B} & \cdots & \cdots & O \\ \vdots & -\tilde{A} & -\tilde{B} & I & -\tilde{B} & \vdots \\ \vdots & \vdots & \vdots & \vdots & \vdots & \vdots \\ O & \cdots & -\tilde{A} & -\tilde{B} & I & -\tilde{B} \end{bmatrix}$$

Using the Schur Complement to solve the KKT system

$$H^{(i)}\triangle\underline{s}_{nt}^{(i)} + A_s^T w = -\underline{r}^{(i)} \tag{13}$$

1) Define $C = -A_s[H^{(i)}]^{-1}A_s^T$
2) Solve for $\underline{w}$ from $C\underline{w} = A_s[H^{(i)}]^{-1}\underline{r}^{(i)}$
3) Solve for $\triangle\underline{s}_{nt}^{(i)}$ from $H^{(i)}\triangle\underline{s}_{nt}^{(i)} = -A_s\underline{w} - \underline{r}^{(i)}$
4) Validation: define $\lambda(\triangle\underline{s}_{nt}^{(i)}) = \sqrt{[\triangle\underline{s}_{nt}^{(i)}]^T H^{(i)}\triangle\underline{s}_{nt}^{(i)}}$

- IF $\frac{1}{2}\lambda^2(\triangle\underline{s}_{nt}^{(i)}) \leq \epsilon$ DO $\underline{s}^{(i+1)} = \underline{s}^{(i)} + \triangle\underline{s}_{nt}^{(i)}$
- ELSE DO *Linear Search*

  Choose $\mu \in (0, 0.5)$ $\eta \in (0, 1)$ $\nu = 1$
  While $\lambda(\underline{s}^{(i)} + \nu\triangle\underline{s}_{nt}^{(i)}) > \lambda(\underline{s}^{(i)}) + \mu\nu\nabla\lambda^T(\underline{s}^{(i)})\triangle\underline{s}_{nt}^{(i)}$
  Do $\nu := \nu\eta$
  Update $\underline{s}^{(i+1)} = \underline{s}^{(i)} + \nu\triangle\underline{s}_{nt}^{(i)}$

V. Results

The simulations are based on the simplified sway model defined in Eqn (10) using Peterka's body parameters [19] as shown in Table I. Four different optimal control problems were solved and their operation simulated for different scenarios.

Table I
Body Characteristics and Dimensionless Model Parameters

Symbol	Quantity	Value
M	Body mass	$76\ kg$
I_0	Body moment of inertia	$66\ kg.m^2$
h	CM height over ankle joint axis	$0.87\ m$
g	Acceleration of gravity	$9.8\ m/s^2$
α	mgh/I_0	9.26
β	$\sqrt{h/g}$	0.092

A. Open-loop Control for Different Initial States without Noise

We first solved the basic postural optimal control problems under no disturbance torque with $J(\underline{x}, \hat{u}) = \sum_0^N [px_1^{2m}(k) + qx_2^{2n}(k) + \hat{u}^2(k)]$, with $[m, n]$=[1, 1], [1, 2], [2, 1] and [2, 2]. The optimal control is open loop, so each problem was solved for every initial condition in a grid as indicated in Table II.

Table II
Open-loop Simulation Parameters

Symbol	Quantity	Values
F_{x_1}	Feasible angular range	$[-5°,\ 5°]$
σ_{x_1}	Angular step interval size	$0.05°$
F_{x_2}	Feasible velocity range	$[-1.5°/s,\ 1.5°/s]$
σ_{x_2}	Velocity step interval size	$0.005°/s$
N	Ending point	20
i	Num of iterations	20
p	Angular cost coefficient	0.1
q	Velocity cost coefficient	0.5

This array consisted of the following feasible sway range: angular displacement $x_1 \in F_{x_1} \triangleq [-5°,\ 5°]$ with step interval size $\sigma_{x_1} = 0.05°$ and angular velocity $x_2 \in F_{x_2} \triangleq [-1.5°/s,\ 1.5°/s]$ with step interval size $\sigma_{x_2} = 0.005°/s$. The resulting optimal state trajectories are shown in Fig. 2.

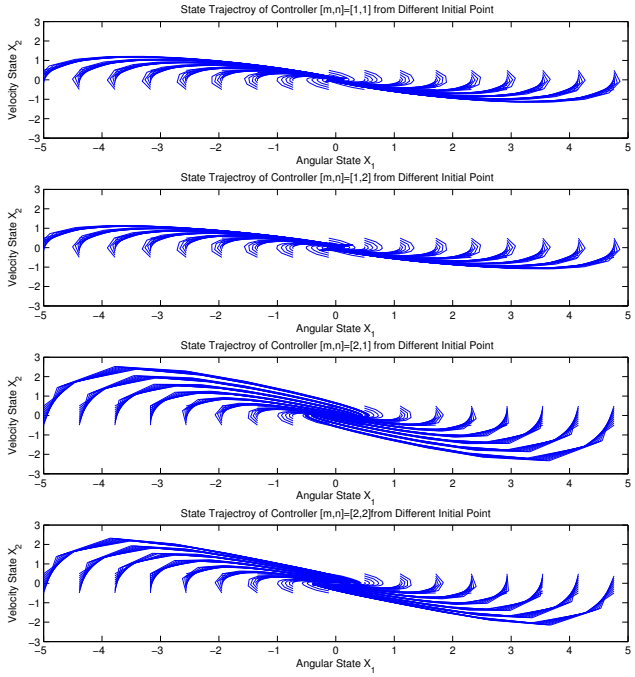

Figure 2. State Trajectory of Four Different Control Strategies Starting from Different Initial State

The $[1, 1]$ result is for an LQ optimal control—a linear system. The $[2, n]$ results, as expected, have considerably more movement for small x_1. The choice of $p = 0.1$ means that the main sway effects will appear for $|x_1| < 0.5°$. In order to obtain an approximation to the optimal feedback control, we then interpreted the first value of the control signal as the optimal feedback gain for any state identical to the initial state, resulting in the control torque as a function of state (feedback control) shown in Fig. 3. The feedback control for an arbitrary initial condition was then computed by interpolating from this grid.

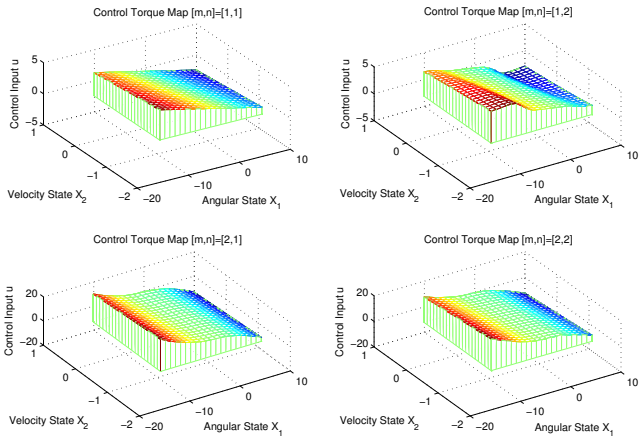

Figure 3. Control Torque Map in the Feasible Sway Range

As expected, the $[1, 1]$ feedback control is linear—it is the LQ optimal feedback control. The other three feedback controls have nearly zero slope at $|x_1| = 0$ and steep slope

for large $|x_1|$. The $[1,2]$ feedback controller seems to have an interesting skewness. We can use the obtained control torque map over the feasible sway range to fully describe the HO system with fixed noise level as is discussed in the following sections.

B. Control with Fixed Initial State and Noise Level

In this section, we simulated the closed–loop HO system with a fixed noise level using the optimal feedback control obtained from the torque map in Fig 3. The noise is white Gaussian noise with zero-mean and standard deviation $\delta_\epsilon = 0.1$. The simulation parameters are listed in Table III.

Table III
FIXED INITIAL STATE AND NOISE LEVEL PARAMETERS

Symbol	Quantity	Value
x_1	Angular displacement	$+3°$
x_2	Angular velocity	$+0.1°/s$
δ_ϵ	Noise level	0.1
T	Simulation duration	$20\ secs$
$\frac{1}{\tau}$	Sampling rate	$50\ Hz$

Notice that the optimal controls for all three HO performance criteria are much more aggressive in reducing the large initial deviations than the LQ optimal control. However, all three respond less to the small deviations that remain after roughly 10 seconds as shown in Fig 4.

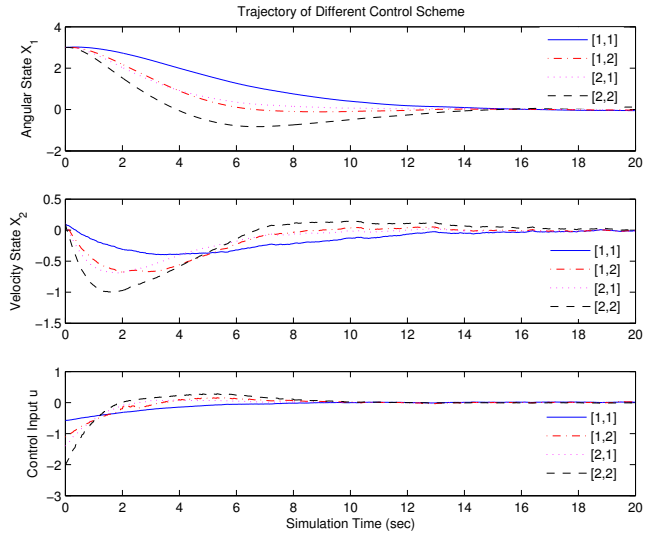

Figure 4. Trajectories of angular state x_1, angular velocity x_2 and the control input $\hat{u}$ for different performance criteria

C. Control of Equilibrium Driven by Different Noise Levels

It is interesting to simulate the system starting from an equilibrium state and driven by different levels of noise. The results are shown in Figs 5 and 6. Note that the noise sequences are identical for all four trajectories in each of the figures. The noise in each figure is, except for a scale factor, also identical. As expected, all of the HO controllers result in greater sway than the LQ optimal controller. Somewhat surprisingly, all four controllers produce trajectories that seem to cluster near some nominal state, drift from that state, and then cluster elsewhere. The $[2,n]$ controllers have the most sway, The $[1,2]$ controller seems to have the least.

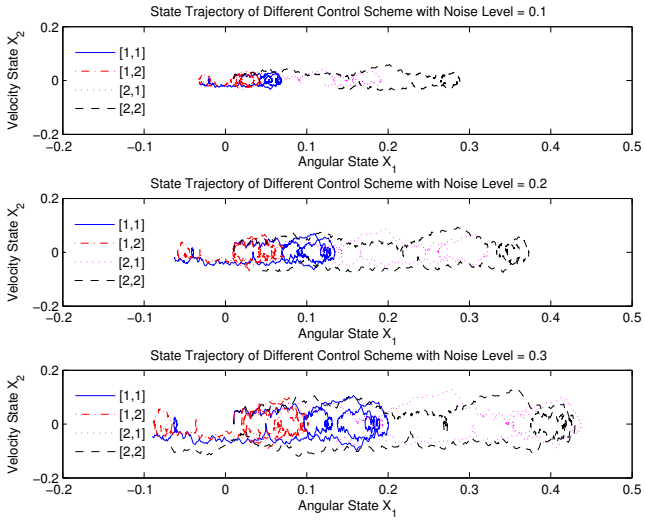

Figure 5. State trajectories of four different control schemes to maintain the equilibrium state driven by different levels of noise

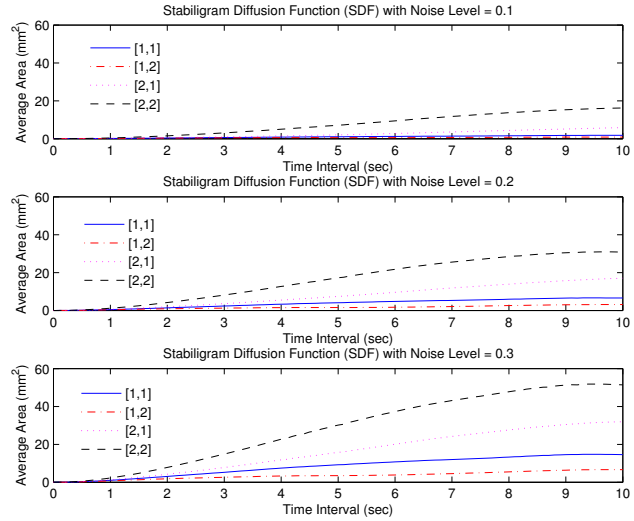

Figure 6. SDF function of four different control schemes to maintain the equilibrium state driven by different levels of noise

The SDF describes the relationship between the time interval of motion and the average of corresponding changes in position [5]. It is sufficient to detect differences in postural sway and also very sensitive. The CP SDF is defined to be $\left\langle \triangle y_p^2 \right\rangle = \left\langle [y_p(t+\triangle t) - y_p(t)]^2 \right\rangle$, where $\langle \cdot \rangle$ denotes the ensemble mean of the time series, and $\triangle t$ ranges from 0 to 10 seconds in the simulation. The computation of y_p, the displacement of the CP is based on the displacement of the CG y_g and CG acceleration $\ddot{y}_g$: $I_0 \ddot{y}_g = Mgh(y_g - y_p)$. At

$\triangle t = 0$, the SDF $\langle \triangle y_p^2 \rangle$value is always zero, when $\triangle t$ increases $\langle \triangle y_p^2 \rangle$ will also increase, because $y_p(t)$ and the time-shifted version $y_p(t+\triangle t)$ becomes less similar to each other.

The SDFs for the four designed control schemes are plotted in figure 6. They demonstrated that the $[1,1]$ controller expends the most energy and the $[2,2]$ the least. Note that stability is not an issue. None of the controllers allows enough sway to jeopardize stability in any way. The conditions for the SDF's plotted in Fig.6 are the standard ones. That is, the subjects start at equilibrium. In this case only the $[2,2]$ controller truly replicates the experimentally obtained SDF's. There is a scaling issue here. The effect of changing p and q on the SDF should be studied. Lastly, we computed the energy expended by each of the controllers in maintaining the posture when starting from equilibrium and perturbed by white Gaussian noise. The results are shown in Table IV.

Table IV
TORQUE ENERGY $E_{ab}(\hat{u}) = \sum_a^b \hat{u}^2(n)$ AT RANGE $[0s, 20s]$OF FOUR CONTROL STRATEGIES UNDER DIFFERENT NOISE LEVEL

Noise level	$[1,1]$	$[1,2]$	$[2,1]$	$[2,2]$
$\delta\epsilon = 0.1$	0.3715	0.1401	0.1998	0.1081
$\delta\epsilon = 0.2$	0.9125	0.5518	0.5565	0.4341
$\delta\epsilon = 0.3$	1.6074	1.1965	1.0966	0.9793

The SDF's measured by Collins [5] and studied by Peterka [19] are similar to those we obtained for our $[1,2]$ and $[2,2]$ optimal controllers. They exhibit two slopes with the steeper slope at small time intervals. Note that the SDF's calculated for $[1,1]$ and $[2,1]$ are nearly straight — different from the experimental observations. The comparison is not completely fair because we have small noise and non-zero initial error. However, the experimental results could possibly begin with some initial error.

VI. CONCLUSIONS

An optimal control problem consisting of a simple dimensionless inverted pendulum model of the human and a performance criterion that is quartic in at least some states and quadratic in the control has been formulated, solved by the Newton-KKT method, and shown, in many respects, to exhibit similar behavior to humans standing quietly. Although the simple inverted pendulum model is standard in the literature on human postural regulation, the greatest value of the work reported here may well be the ease with which it can be extended. Optimal control models of the quietly standing human involving more complex models of the human and performance criteria of the form of Eqn. (1) can be solved by the same techniques as were used in this paper.

This approach provides an effective way to study, among other aspects of the control problem, the coordination of muscles acting at the knee, hip, and ankles. This approach can even handle delays, although with the somewhat unrealistic restriction that the full state is available to the controller. Because the dynamics are linear, the excursions from equilibrium are small and the performance criteria are symmetric about zero, certainty equivalence is likely to hold, at least approximately. Thus, this approach can be used to study the effects of delay.

REFERENCES

[1] Accornero N, Capozza M, and Manfredi GW. Clinical multisegmental posturography: age-related changes in stance control. Electroenceph Clin Neurophysiol 105: 213-219, 1997.

[2] Aramaki Y, Nozaki D, Masani K, Sato T, Nakazawa K, and Yano H. Reciprocal angular acceleration of the ankle and hip joints during quiet standing in humans. Exp Brain Res 136: 463-473, 2001.

[3] S.P. Boyd and L. Vandenberghe. Convex Optimization. Cambridge University Press,2003 Material available at http://www.stanford.edu/~ boyd/cvxbook.html

[4] Collins JJ and DeLuca CJ. The effects of visual input on open-loop and closed-loop postural control mechanisms. Exp Brain Res 103: 151-163, 1995.

[5] Collins JJ and DeLuca CJ. Open-loop and closed-loop control of posture: a random-walk analysis of center-of-pressure trajectories. Exp Brain Res 95: 308-318, 1993.

[6] Collins JJ and DeLuca CJ. Random walking during quiet standing. Phys Rev Lett 73: 764-767, 1994.

[7] Fitzpatrick R and McCloskey D. Proprioceptive, visual and vestibular thresholds for the perception of sway during standing in humans. J Physiol 478: 173-186, 1994a

[8] Fitzpatrick R, Rogers DK, and McCloskey DI. Stable human standing with lower-limb muscle afferents providing the only sensory input. J Physiol 480: 395-403, 1994

[9] Jeka JJ, Schöner G, Dijkstra T, Ribeiro P, and Lackner JR. Coupling of fingertip somatosensory information to head and body sway. Exp Brain Res 113(3): 475–483, 1997

[10] Jeka JJ, Ribeiro P, Oie KS, and Lackner JR. The structure of somatosensory information for human postural control. Motor Control 2(1): 13–33, 1998

[11] Jeka JJ, Oie KS, and Kiemel T. Multisensory information for human postural control: integrating touch and vision. Exp Brain Res. 134(1): 107–125, 2000

[12] Joseph J and Nightingale A. Electromyography of muscles of posture: leg muscles in males. J Physiol 117: 484-491, 1952

[13] Kuo AD. An optimal control model for analyzing human postural balance. IEEE Trans Biomed Eng 42: 87–101, 1995.

[14] Loram ID and Lakie M. Direct measurement of human ankle stiffness during quiet standing: the intrinsic mechanical stiffness is insufficient for stability. J Physiol 545(3): 1041–1053, 2002

[15] Lacour M, Barthelemy J, Borel L, Magnan J, Xerri C, Chays A, and Ouaknine M. Sensory strategies in human postural control before and after unilateral vestibular neurotomy. Exp Brain Res 115: 300-310, 1997.

[16] Mauritz KH and Dietz V. Characteristics of postural instability induced by ischemic blocking of leg afferents. Exp Brain Res 38: 117-119, 1980

[17] Morasso P and Schieppati M. Can muscle stiffness alone stabilize upright standing? J Neurophysiol 83: 1622–1626, 1999.

[18] Peterka RJ and Benolken MS. Role of somatosensory and vestibular cues in attenuating visually induced human postural sway. Exp Brain Res 105: 101–110, 1995.

[19] Peterka RJ. Postural control model interpretation of stabilogram diffusion analysis. Biol Cybern. 82: 335–343, 2000

[20] Smith JW. The forces operating at the human ankle joint during standing. J Anat 91: 545-564, 1957

[21] Winter DA, Patla AE, Prince F, Ishac M, and Gielo-Perczak K. Stiffness control of balance in quiet standing. J Neurophysiol 80: 1211-1221, 1998

[22] Winter DA, Patla AE, Rietdyk S, and Ishac MG. Ankle muscle stiffness in the control of balance during quiet standing. J Neurophysiol 85: 2630-2633, 2001.